SANDIA REPORT

SAND2003-8517
Unlimited Release
Printed September 2003

Development of Porous Polymer Monoliths for Reverse-Phase Chromatography of Proteins

C.P. Stephens and T.J. Shepodd

Prepared by
Sandia National Laboratories
Albuquerque, New Mexico 87185 and Livermore, California 94550

Sandia is a multiprogram laboratory operated by Sandia Corporation,
a Lockheed Martin Company, for the United States Department of Energy's
National Nuclear Security Administration under Contract DE-AC04-94AL85000.

Approved for public release; further dissemination unlimited.

Issued by Sandia National Laboratories, operated for the United States Department of Energy by Sandia Corporation.

NOTICE: This report was prepared as an account of work sponsored by an agency of the United States Government. Neither the United States Government, nor any agency thereof, nor any of their employees, nor any of their contractors, subcontractors, or their employees, make any warranty, express or implied, or assume any legal liability or responsibility for the accuracy, completeness, or usefulness of any information, apparatus, product, or process disclosed, or represent that its use would not infringe privately owned rights. Reference herein to any specific commercial product, process, or service by trade name, trademark, manufacturer, or otherwise, does not necessarily constitute or imply its endorsement, recommendation, or favoring by the United States Government, any agency thereof, or any of their contractors or subcontractors. The views and opinions expressed herein do not necessarily state or reflect those of the United States Government, any agency thereof, or any of their contractors.

Printed in the United States of America. This report has been reproduced directly from the best available copy.

Available to DOE and DOE contractors from
U.S. Department of Energy
Office of Scientific and Technical Information
P.O. Box 62
Oak Ridge, TN 37831

Telephone: (865)576-8401
Facsimile: (865)576-5728
E-Mail: reports@adonis.osti.gov
Online ordering: http://www.doe.gov/bridge

Available to the public from
U.S. Department of Commerce
National Technical Information Service
5285 Port Royal Rd
Springfield, VA 22161

Telephone: (800)553-6847
Facsimile: (703)605-6900
E-Mail: orders@ntis.fedworld.gov
Online order: http://www.ntis.gov/help/ordermethods.asp?loc=7-4-0#online

SAND2003-8517
Unlimited Release
Printed September 2003

Development of Porous Polymer Monoliths for Reverse-Phase Chromatography of Proteins

Christopher P. Stephens
Timothy J. Sheppod
Materials Chemistry Department
Sandia National Laboratories
P.O. Box 5800
Albuquerque, New Mexico 87185-9403

ABSTRACT

The polymers developed in this project are intended for use as a stationary phase in reverse-phase chromatography of proteins, where the mobile phase is a solution of acetonitrile and a phosphate buffer, 6.6 pH. A full library of pore sizes have been developed ranging from 0.41μm to 4.09 μm; these pore sizes can be determined by the solvent ratio of tetrahydrofuran:methoxyethanol during polymerization. A column that can separate proteins in an isocratic mode would be a vast improvement from the common method of separating proteins through gradient chromatography using multiple solvents. In the stationary phase, the main monomers have hydrophobic tails, lauryl acrylate and steryl acrylate. Separations of small hydrophobic molecules and peptides (trial molecules) have efficiencies of 24,000-33,000 theoretical plates m^{-1}. The combination of a highly non-polar stationary phase and a mobile phase where the polarity can be controlled provide for excellent separation.

Intentionally Left Blank

CONTENTS

TABLES

Development of Porous Polymer Monoliths for Reverse–Phase Chromatography of Proteins

I. Introduction

Reverse-Phase Chromatography

Reverse-phase chromatography (RPLC) is made up of a mobile phase (solvent) and stationary phase. The differential solute/stationary phase interactions provide separation of the solute molecules by hydrophobic interactions and polar forces i.e., hydrogen bonding and dipole-dipole interactions.[1] The efficiency of the column can be controlled by modifying the polarity of the stationary and mobile phase or by changing the salt concentration in the mobile phase.[2,3] Sensitive separations using column electrochromatography (CEC) technique, which can detect volume less than one nanoliter.[4]

Electroosmotic Flow

In our columns, the mobile phase moves by an electroosmotic flow (EOF), which is induced by a voltage difference between the ends of the column. Our columns are negatively charged, so when the voltage is applied the mobile cations move toward the anode, which also causes the mobile phase to be dragged toward the anode with the cation.[5] The higher the voltage the faster the separation and the time allowed for diffusion is minimized. When a column is operated under EOF the efficiency is determined by equation 1, where N is the number of theoretical plates, V is the applied voltage, D is the molecular diffusion coefficient, and μ is the electrophoretic mobility [6].

$$N = \frac{\mu V}{2D} \qquad 1$$

Equation 1 shows the efficiency of a column flowing under EOF is independent of the column length and is directly dependant on the applied voltage.[6] Another important feature of separation under EOF is that the flow profile is flat instead of parabolic like in High-Performance-Liquid-Chromatography; this flat-flow profile improves the efficiency of the chromatography column.[5]

Stationary Phase

The stationary phase of the column is composed of a porous polymer monolith (PPM), fabricated by polymerization-induced phase separation.[7,8] The pore size of these PPMs are determined by the solvent strength.[8,9] The PPM has an advantage over the traditional bead packed columns (common in the HPLC technology), which is that they can conform to the shape of the chromatography device.[8] This development of PPMs provides for cheaper and more reproducible device fabrication. Pretreatment of the capillary walls binds the stationary phase to the inner wall of the glass capillary.

Hydrophobic Interactions

The addition of a hydrophobic solute to an aqueous mobile phase induces ordering within the water molecules, leading to exclusion of the hydrophobic material from the mobile phase on a hydrophobic stationary phase.[2,8] The hydrophobicity of a protein is dependant on the sum of all amino acid hydrophobicities either on the surface or buried within the folded proteins.[2] By modification of either the salt compositions or the salt concentration in the mobile phase, the polarity of the mobile phase can be modified.[2] An increase in the polarity of the mobile phase (often represented by an increase in the water concentration in an acetonitrile/aqueous mobile phase) will lead to an increase in the retention time of the hydrophobic proteins.

II. Methods

Column Preparation

The fused silica capillaries used have an inner diameter of 103 μm (Polymicro Technologies). The columns are given a negative pretreatment, so that the polymers attach to the inner walls of the column. This pretreatment is composed of deionized water (50%), acetic acid (30%) and z-6030 (20%) that is placed into the capillary for several hours and rinsed clean. This negative pretreatment on the inside of the column matches the charge of the mobile phase, as to improve the EOF of the column.

Polymerization

The prepolymer solution is 33% monomer, 60% solvent, and 7% buffer (10 mM phosphate buffer, 6.6 pH). The monomers are composed of hydrophobic lauryl acrylate (Table 1A, 27.3%) and steryl acrylate (Table 1B, 27.3%); crosslinker 1,4 butanediol diacrylate (Table 1C, 27.3%), tetrahydrofurfuryl acrylate (Table 1D, 18.2%), and negative charge carrier 2-Acrylamido-2-methyl-1-propanesulfonic acid, AMPS (Table 1E, 1 wt% of monomers).

Table 1: Monomers

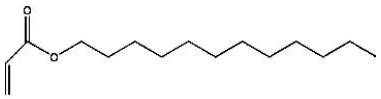

A) Lauryl Acrylate

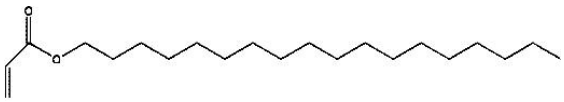

B) Steryl Acrylate

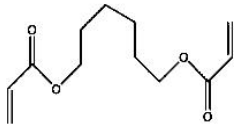

C) 1,4 Butanediol Diacrylate

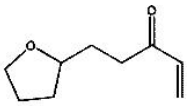

D) Tetrahydrofurfuryl Acrylate

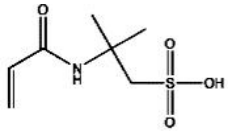

E) 2-Acrylamido-2-Methyl-1-Propanesulfonic Acid

The solvent used is methoxyethanol (X%) and tetrahydrofuran (Y%), where the composition is described in Table 2.

Table 2: Solvent Composition Variations

Sample	Designation	Methoxyethanol, ME (%), X	Tetrahydrofuran, THF (%), Y	THF:ME
A	30TS88A	23.8	76.2	3.20
B	30TS87A	30.0	70.0	2.33
C	30TS86A	38.5	61.5	1.60
D	28TS150A	45.2	54.8	1.21
E	30TS97A	51.3	48.7	0.95
F	30TS97B	61.5	38.5	0.63
G	30TS98A	66.7	33.3	0.50
H	30TS98B	72.7	27.3	0.38

The polymerization is initiated with 2,2'-azobisisobutyronitrile, AIBN (0.5 wt% of total solution). Initiation of the AIBN was accomplished using an UV curing oven (Spectrolinker XL-1500) at 365 nm (Spectronics Corp. BLE-1T151 Bulbs) for 30 minutes. After the AIBN has been initiated and the polymerization reaction has begun the column is allowed to set for 15 hours to allow adequate time for the completion of the polymerization reaction. The

column is then flushed with 70% tetrahydrofuran and 30% phosphate buffer for 6 hours followed by the mobile phase used for chromatography for 6 hours at 1700 psi.

Pore-Size Characterization

Soxhlet Extraction using methanol was performed on the samples for 6 hours followed by a 3 hour of drying at 70 ^{o}C period to remove the methanol. After the samples have completed the extraction and drying protocol they are ready for SEM or mercury porosimetry. JEOL 6400F Field Emission Scanning Electron Microscope (SEM) was used for visual characterization of PPM pore size at 4 kV (a Au/Pd coating was placed on the samples for 90 seconds at 10 mA and 90 seconds at 20 mA). The SEM is useful in determining particle size, which is proportional to pore size (an increase in particle size leads to an increase in pore size). In order to get at the pore size directly, mercury porosimetry must be utilized. Mercury porosimetry works on the fact that mercury is a non-wetting material, it must be forced into the pores of a porous material with a given applied pressure.[10] As the pressure applied to the mercury increases, it is able to move into smaller diameter pores, by knowing the volumetric change and the pressure difference the distribution of pore sizes can be determined (Mercury Porosimetry).[10] Mercury porosimetry and single-point krypton BET analyses were performed by Porous Materials, Inc.

Chromatography

A polymer-free window was produced using an Argon laser (257 nm) at a power setting of 25 A (Coherent Innova 300 FRED) with a continual flow of running solution at 1882 psi. Both ends of the column are placed in the running solution, then a specific voltage is placed across the column. The column is then aligned in the detector (Linear UVIS 200) so that the window in the column is located above the UV-beam of the detector. The detector is set to operate at 214 nm. For a given separation, the number of theoretical plates (plates m^{-1}) can be determined by the equation 2,

$$N = \frac{16 * \left(\frac{t_R}{w_b} \right)^2}{CL} \qquad 2$$

where w_b is the width at the base of the chromatography peak (minutes), t_R is the retention time (minutes), and CL is the column length (m).[3]

Example Method

The following are the steps to making formulation 28TS150A (Sample D).

Step 1:
Flow the negative pretreatment solution (10 mL DI water, 6 mL acetic acid, and 4 mL z-6030) through the capillary using capillary action. Leave the pretreatment solution in the column for 6 hours. Flush the column with acetonitrile and then clear the column with air.

Step 2:
Mix the prepolymer solution in a separate vial. Mix the solvents (890 μL of ME and 1080 μL of THF) with the Phosphate buffer (240 μL) and the THFA (200 μL). Add the monomers to the vial: 1,4 BDDA (300 μL), LA (300 μL), and SA (300 μL). Add the initiator (10.3 mg of AIBN) and the charged monomer (14.3 mg of AMPS).

Step 3:
Filter the prepolymer mixture with a 0.45-μm pore size PTFE filter into two 1.5 mL vials (fill one vial to the top and the other vial half way to the top). Using a firestone valve and vacuum manifold, cycle three times between acuum (< 1800 mTorr) and nitrogen gas (10 seconds) for degassing the prepolymer. Insert one side of the column into the bottom of the full vial and insert the other side of the column into the half-full vial (don't let the column touch the

prepolymer). Using capillary action, flow the monomer through the capillary. Once a steady flow of prepolymer solution is reached, the second end of the capillary is put into the prepolymer solution.

Step 4:
Put the column and the vials into the UV-Crosslinking oven and polymerize for 1800 seconds using 365-nm bulbs. Let the polymer sit in the vials and column for 9 hours to allow for complete polymerization.

Step 5:
Take the column out of the vials and flush with 70% THF and 30% ACN for 6 hours using a HPLC pump at 1200 psi. Then the column is flushed with the column's mobile phase for 6 hours at 1200 psi. A window is then burned into the column using a 257-nm Argon laser, so that the UV detector used in chromatography has an unobstructed viewing path. The column must be kept in the mobile phase solution to prevent drying out.

Step 6:
The column is placed in the UV detector so that the viewing window is above the detector beam (the column is aligned by moving the column in the detector until the absorbance is minimized). Both ends of the column are placed into the mobile phase solution; a positive electrode is placed in one of the vials of the mobile solution and a negative electrode is placed in the other vial. The voltage is set to 6 kV causing electroosmotic flow to initiate (the measured current if proportional to the flow through the column).

Step 7:
Once the current is stable at a reasonable value, the chromatography can be started. The first step in chromatography is to inject the sample to be studied into the column for a short period of time (10 seconds) using electroosmotic flow. Then place the column back into the mobile phase and initiate the running voltage (6 kV).

III. Results

SEM images of Sample A (Figs. 1 ,9, and 17), Sample B (Figs. 2, 10, and 18), Sample C (Figs. 3, 11, and 19), Sample D (Figs. 4, 12, and 20), Sample E (Figs. 5, 13, and 21), Sample F (Figs. 6, 14, and 22), Sample G (Figs. 7, 15, and 23), and Sample H (Figs. 8, 16, and 24) show the particle sizes of the stationary phase.

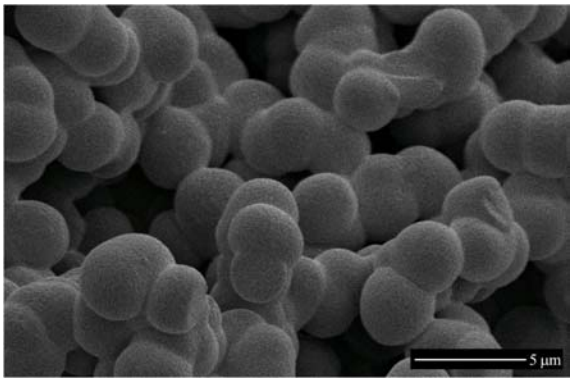

Figure 1: Sample A (Low Magnification)

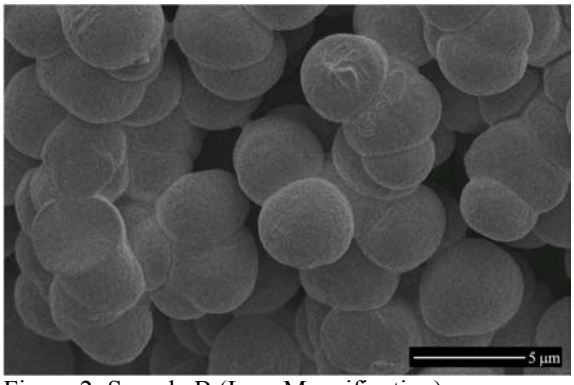

Figure 2: Sample B (Low Magnification)

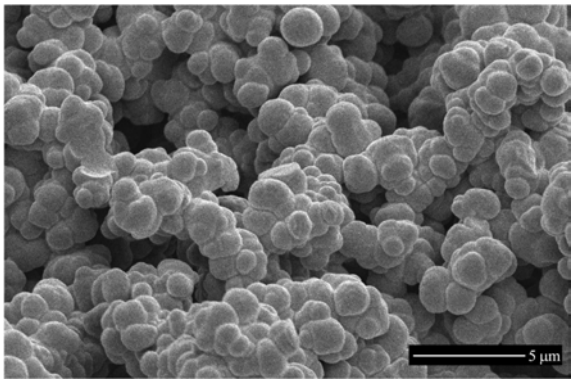

Figure 3: Sample C (Low Magnification)

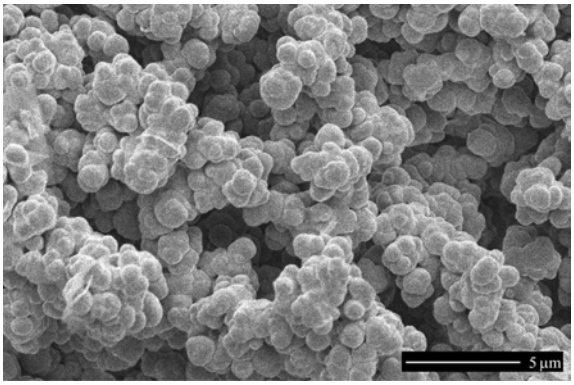

Figure 4: Sample D (Low Magnification)

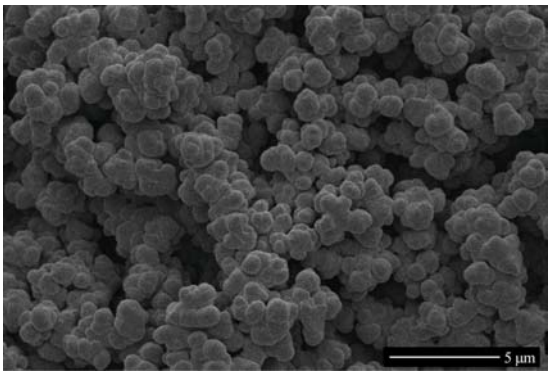

Figure 5: Sampble E (Low Magnification)

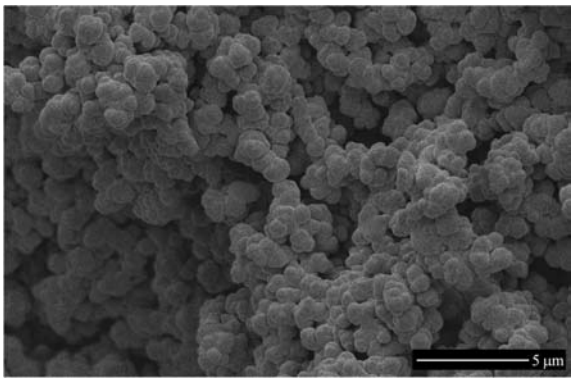

Figure 6: Sample F (Low Magnification)

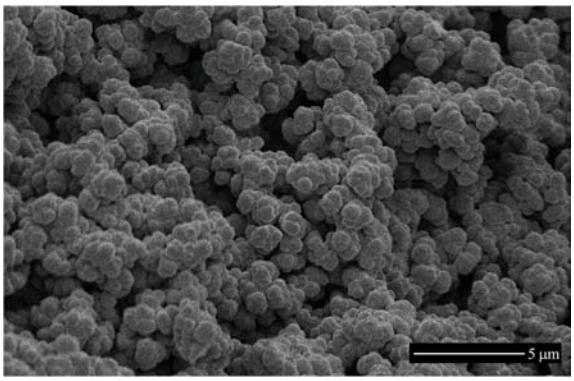

Figure 7: Sample G (Low Magnification)

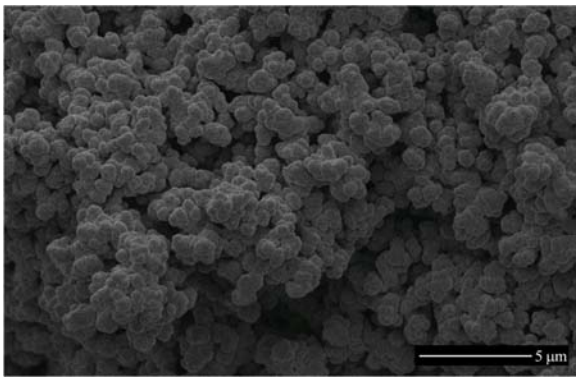

Figure 8: Sample H (Low Magnification)

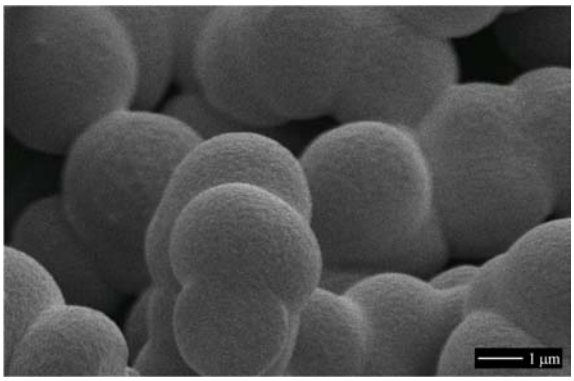

Figure 9: Sample A (Medium Magnification)

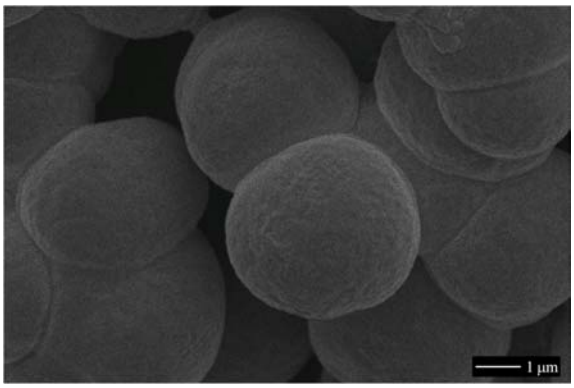

Figure 10: Sample B (Medium Magnification)

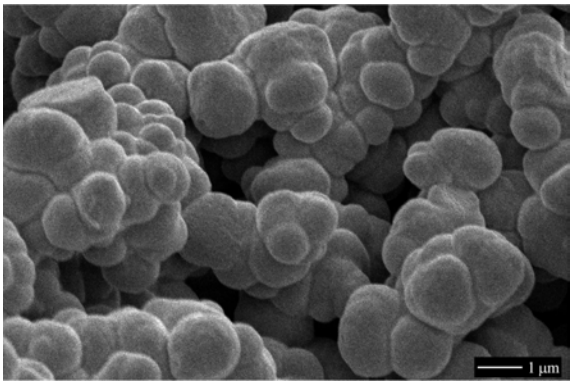

Figure 11: Sample C (Medium Magnification)

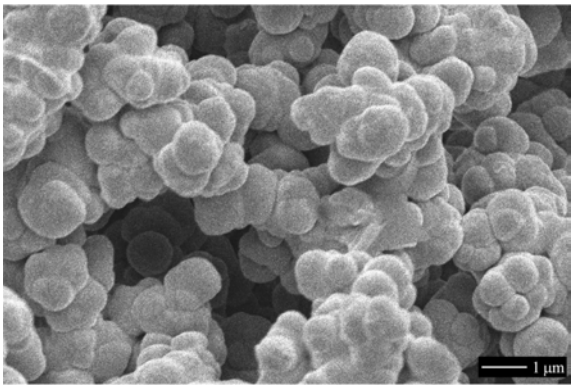

Figure 12: Sample D (Medium Magnification)

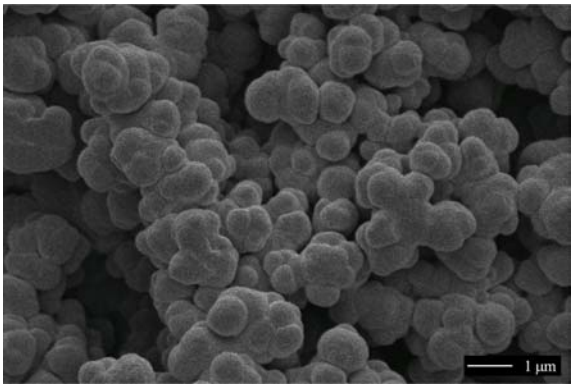

Figure 13: Sample E (Medium Magnification)

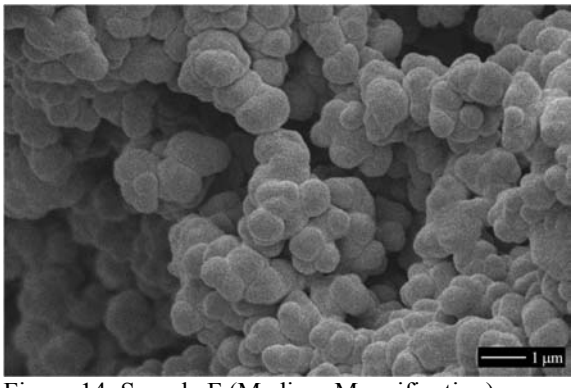

Figure 14: Sample F (Medium Magnification)

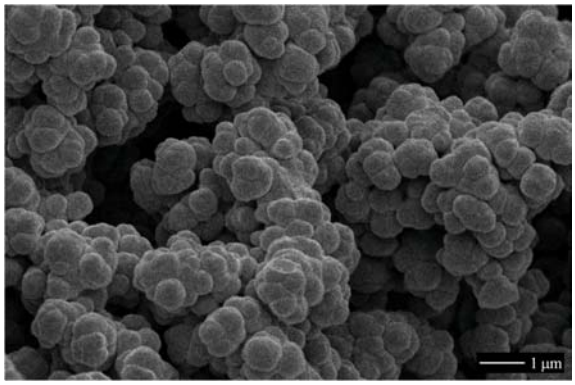

Figure 15: Sample G (Medium Magnification)

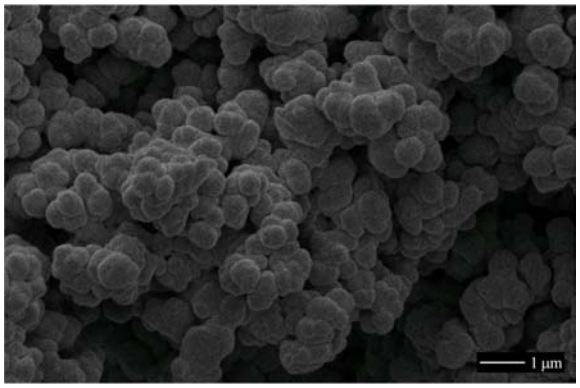

Figure 16: Sample H (Medium Magnification)

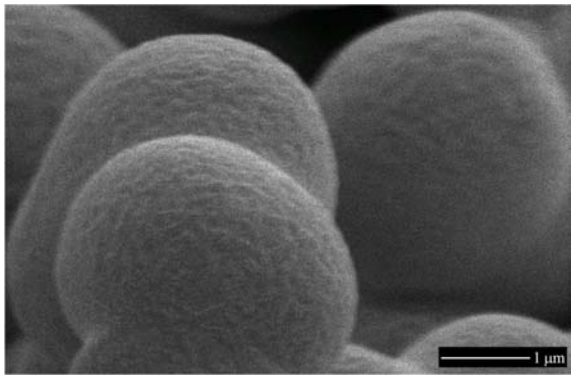

Figure 17: Sample A (High Magnification)

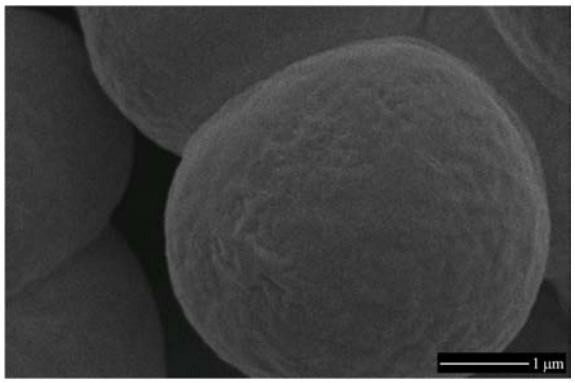

Figure 18: Sample B (High Magnification)

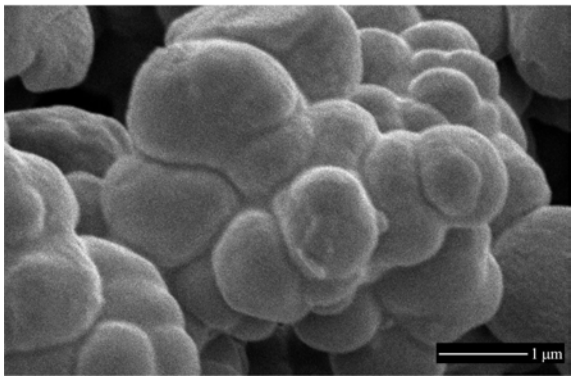

Figure 19: Sample C (High Magnification)

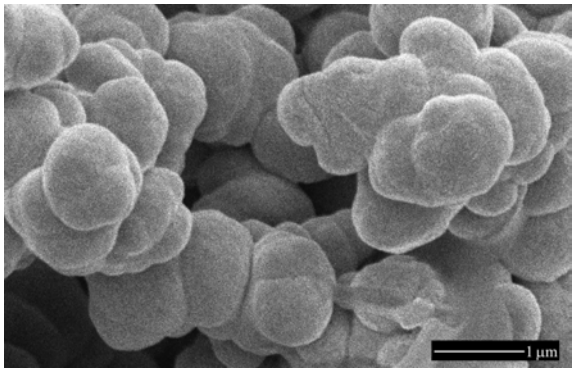

Figure 20: Sample D (High Magnification)

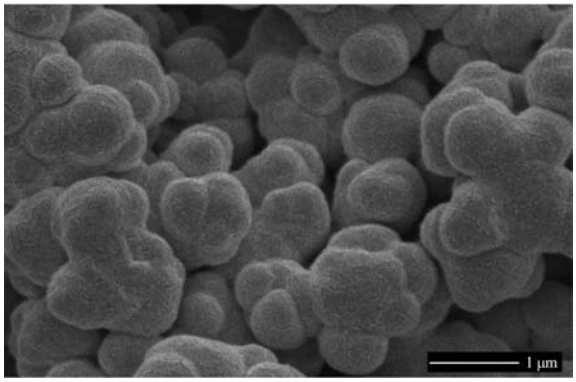

Figure 21: Sample E (High Magnification)

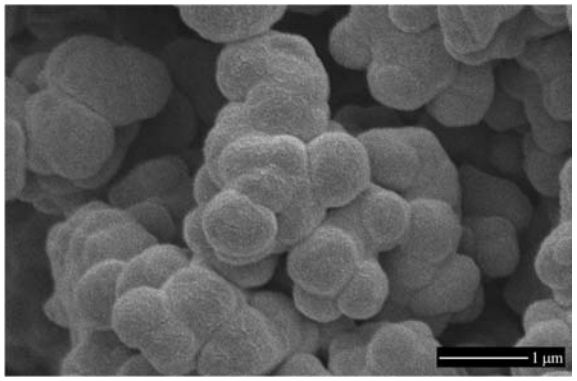

Figure 22: Sample F (High Magnification)

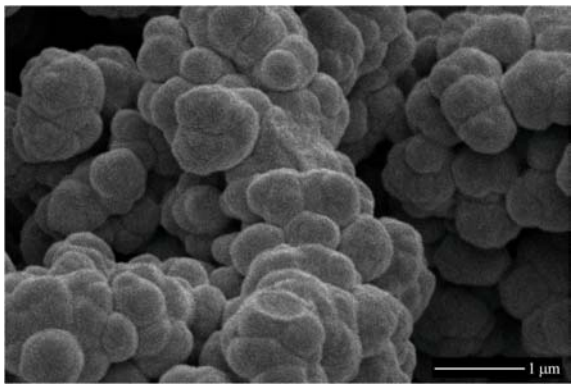

Figure 23: Sample G (High Magnification)

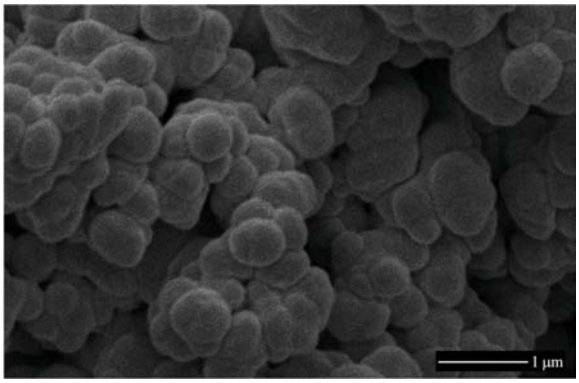

Figure 24: Sample H (High Magnification)

Table 3 shows the particle size of each sample: Sample A is 3.33 ± 0.44, Sample B is 4.09 ± 0.42, Sample C is 1.20 ± 0.29, Sample D is 0.84 ± 0.19, Sample E is 0.67 ± 0.15, Sample F is 0.67 ± 0.13, Sample G is 0.54 ± 0.09, and Sample H is 0.41 ± 0.07. A graphical representation of this data is displayed in Figure 25, which is fit with an exponential curve. The particle size is related to the pore size, so that as the particle size decreases the pore size also decreases. This allows SEM particle size measurements to be used as a relative measure of pore size.

Table 3: Particle size distribution for samples A-H

Sample	Designation	THF:ME	Particle Size (µm)
A	30TS88A	3.20	3.33 ± 0.44
B	30TS87A	2.33	4.09 ± 0.42
C	30TS86A	1.60	1.20 ± 0.29
D	28TS150A	1.21	0.84 ± 0.19
E	30TS97A	0.95	0.67 ± 0.15
F	30TS97B	0.63	0.67 ± 0.13
G	30TS98A	0.50	0.54 ± 0.09
H	30TS98B	0.38	0.41 ± 0.07

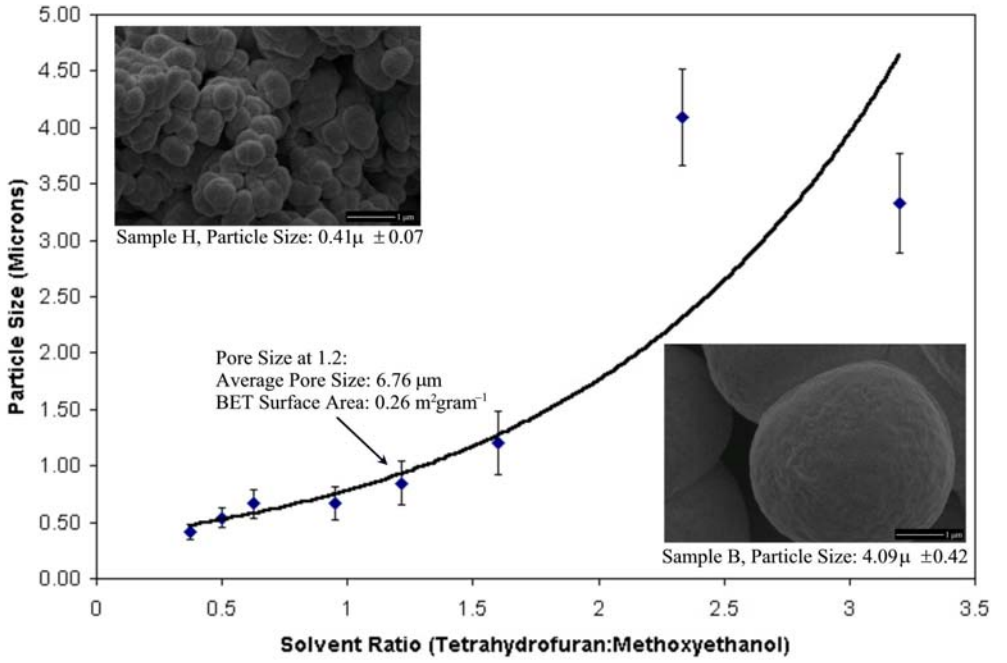

Figure 25: Particle size dependence on solvent ratio

The effect of solvent strength on particle size can be seen in Figure 25; it can be seen that the methoxyethanol is stronger than the tetrahydrofuran, so as the methoxyethanol is increase the particle size gets smaller. A cross-section of a typical chromatography column is shown in Figure 26; the PPM can be seen to attach to the side walls, because of the negative pretreatment with silane. Mercury porosimetry (Figure 27) of sample D shows that the pore size has a large distribution from 0.2-100 µm with a mean around 6.76 µm (based on volume). The single point krypton BET surface area of sample D is 0.260107 m^2 g^{-1}. This surface is consistent with the geometry in the micrographs having little or no nanopores.

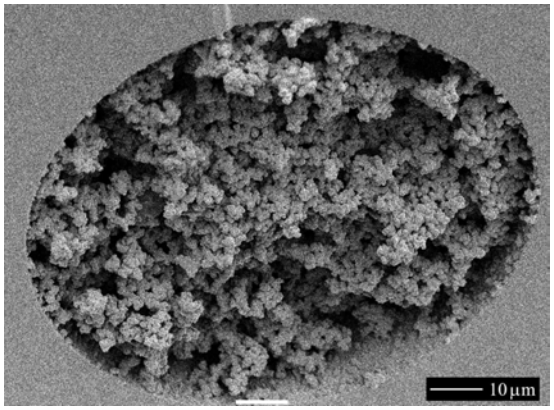

Figure 26: Column Sample D

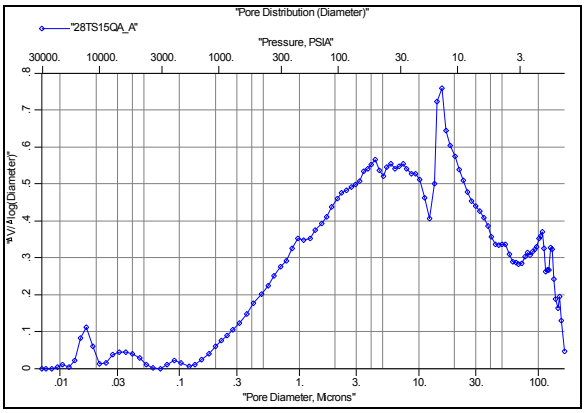

Figure 27: Mercury Porosimetry of Sample D

Figure 28 shows the separation of an HPLC standard (Gly-Tyr, Val-Tyr-Val, Methionine enkepalin, leucine enkephalin and angiotensin II) at three different voltages 9 kV (blue), 6 kV (green), and 3 kV (red). As the voltage decreases the current also decreases, leading to a decrease in EOF. With a slower EOF the peptides have a longer period of time to attach onto the stationary phase, which leads to improved seperation and minimization of diffusion. This can be seen by the improvement of the number of theoretical plates on the column 25,000 plates m^{-1} (blue), 28,000 plates m^{-1} (green), and 33,000 plates m^{-1} (red). The Napthalene peak of the Napthalene/Pyrene/Flourene separation (Figure 29) has an efficiency of 24,000 theoretical plates m^{-1}.

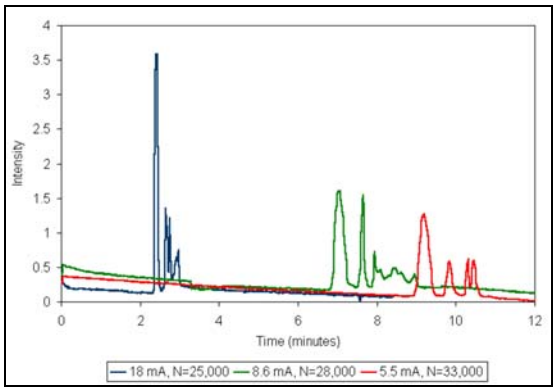

Figure 28: Separation of HPLC Standard on Sample D.

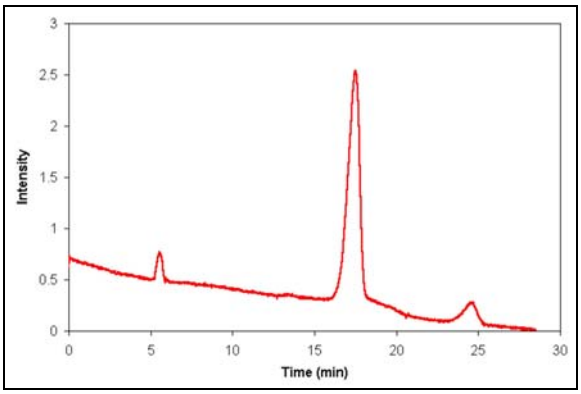

Figure 29: Separation of Flourene/Pyrene/Napthalene on Sample D.

IV. Conclusions

A moderate peptide separation was achieved with the new column formulation, but optimization of the stationary phase must take place in order to improve separation. The typical efficiency of the new separation column is 24,000-28,000 plates m^{-1}; this moderate separation can be explained by the mercury porosimetry data, which show that the average pore size in the monolith is 6.76 μm. The large pore size seen in these columns decreases the amount of contact that the protein has with the stationary phase.

A full library of pore sizes have been developed ranging from 0.41μm to 4.09 μm; these pore sizes can be determined by the solvent ratio of tetrahydrofuran: methoxyethanol. These new columns have not been fully characterized, but the SEM images in this report show the ability to dial the desired pore size into the monomer mixture.

V. Future Work

The work that still remains to be complete on this project is mercury porosimetry (to determine pore size) and chromatography of peptides and proteins.

VI. References

(1) Braithwaite, A.; Smith, F. J. *Chromatographic Methods*; J.W. Arrowsmith Ltd.: Great Britain, 1985.

(2) Queiroz, J. A.; Tomaz, C. T.; Cabral, J. M. S. *Journal of Biotechnology* **2001**, *87*, 143-159.

(3) Krstulovic, A. M.; Brown, P. R. *Reversed-Phase High-Performace Liquid Chromatography*; John Wiley and Sons: New York, 1982.

(4) Yan, C.; Dadoo, R.; Zhao, H.; Zare, R. N.; Rakestraw, D. J. *Anal. Chem.* **1995**, *67*, 2026-2029.

(5) Svec, F.; Peters, E. C.; Sykora, D.; Frechet, J. M. J. *Journal of Chromatography A* **2000**, *887*, 3-29.

(6) Jorgenson, J. W.; Lukacs, K. D. *Anal. Chem.* **1981**, *53*, 1298-1302.

(7) Elicabe, G. E.; Larrondo, H. A.; Williams, R. J. J. *Macromolecules* **1998**, *31*, 8173-8182.

(8) Ngola, S. M.; Fintschenko, Y.; Choi, W.-Y.; Shepodd, T. J. *Anal. Chem.* **2001**, *73*, 849-856.

(9) Yu, C.; Svec, F.; Frechet, J. M. J. *Electrophoresis* **2000**, *21*, 120-127.

(10) Jena, A.; Gupta, K. "Advanced Technology for Evaluation of Pore Structure Characteristics of Filtration Media to Optimize Their Design an Performance," Porous Materials, Inc.

Distribution

1 Chris Stephens
1815 Raven Hill Court
Knoxville, TN 37922

1	MS 9403	Tim Sheppod, 8722
3	MS 9018	Central Technical Files, 8945-1
1	MS 0899	Technical Library, 9616
1	MS 9021	Classification Office, 8511 for Technical Library, MS 0899, 9616
		DOE/OSTI via URL